

## Numerical modeling of the winter circulation of the Gulf of Trieste (northern Adriatic)

Vlado MALAČIČ and Boris PETELIN

*National Institute of Biology, Marine Biology Station, 6330 Piran, Slovenia*

---

*Numerical simulations of the winter circulation in and around the Gulf of Trieste are presented. The model, based on the architecture of the Princeton Ocean Model, gave reasonable results for circulation in the Gulf during the winter period, when the dominant bora wind is blowing. Three model runs with different initial and surface boundary conditions show that there is an outflow along the shallow northern coastline of the Gulf and over the surface of the major part of the area, and an inflow at depth in the central and southern parts of the Gulf. However, the variability of the temperature and salinity fields when vertical fluxes of heat and salinity are present cause a weak outflow in an area near the southern part of the Gulf, and make the general circulation pattern more complex.*

---

**Key words:** Adriatic Sea, Gulf of Trieste, numerical modeling, coastal dynamics, wind-driven dynamics

### INTRODUCTION

From sporadic and instantaneous current-meter observations that were conducted during the years 1951-55 and 1980-82, in more or less stable (windless) weather conditions near the closed eastern side of the Gulf of Trieste, STRAVISI *et al.* (1981) plotted a sketch of the residual circulation in the Gulf in which a cyclonic gyre near the bottom was observed, as was an anticyclonic gyre at the surface, with a sharp vertical gradient of speed near the surface (STRAVISI, 1983). The effect of horizontal density gradients on the velocity was not considered. However, during the winter of 1984-1985, when the bora (ENE) wind was the dominant forcing agent, observations at the northern side and in

the eastern part near the closed end of the Gulf (MOSETTI & PURGA, 1983; MOSETTI & MOSETTI, 1990) showed that the surface wind-driven current reached a speed of 0.03 times the wind speed measured in Trieste and that at a depth of 6 m the current speed was of 0.02 times the wind speed. MOSETTI & MOSETTI (1990) have shown that during the bora wind, which can reach gusts of more than  $30 \text{ ms}^{-1}$ , there is a water outflow from the Gulf at the surface, an inflow at depth and strong vertical mixing between the surface and deeper parts of the water column. No counter-current was observed, except at a station at the south-eastern closure of the Gulf (their station 'A'). Previous studies were thoroughly overviewed elsewhere (MALAČIČ & PETELIN, 2001), in which current-meter observations

during spring 1999, representative of a flow through the southern side of the entrance into the Gulf of Trieste, were analysed. It was shown that for a dominant inflow into the Gulf a three layer structure was present (surface, intermediate and bottom layers), with a typical EKMAN spiral in the intermediate layer, with a clockwise turn of direction and with a decrease of speed with depth.

We also know about the circulation along the southern side of the interior of the Gulf of Trieste during winter, since the data from the coastal oceanographic buoy near Piran (COSP) were analysed for this situation. During January 2003 there was a period of long-lasting bora wind and we observed a typical situation: an outflow from the Gulf at the surface, and an inflow at depth along the southern (Slovenian) coastline. It was expected that along the northern (Italian) coastline of the Gulf, which is shallower, there would be mainly an outflow. This paper presents the results of an ACOAST-2 model during a winter period (first ten days of a perpetual year) for three cases of different initial conditions and model forcing. The basic hypothesis is explored

that during the winter time there is an inflow of the water mass at depth along the southern coastline into the Gulf, and an outflow along the northern (Italian) coastline.

## THE NUMERICAL MODEL

The Princeton Ocean Model (POM) was applied for the study of the circulation of the Gulf of Trieste, a semi-enclosed basin situated in the shallow northernmost part of the Adriatic Sea. Since the goal of the circulation study was to examine the exchange of the water mass of the small Gulf (that is about 20 km x 20 km in size) a larger model domain was chosen (Fig. 1).

The horizontal resolution of the model is 0.5 km and the model is one-way nested in the coarser ASHELF-1 (nesting) model (ZAVATARELLI & PINARDI, 2003) that roughly covers the area north of the line Ancona-Pula and has a resolution of 1.5 km. The ASHELF-1 model is run by Istituto Nazionale di Geofisica e Vulcanologia (INGV) in Bologna. The model presented in Fig. 1 will be named the ACOAST-1.2 (nested) model

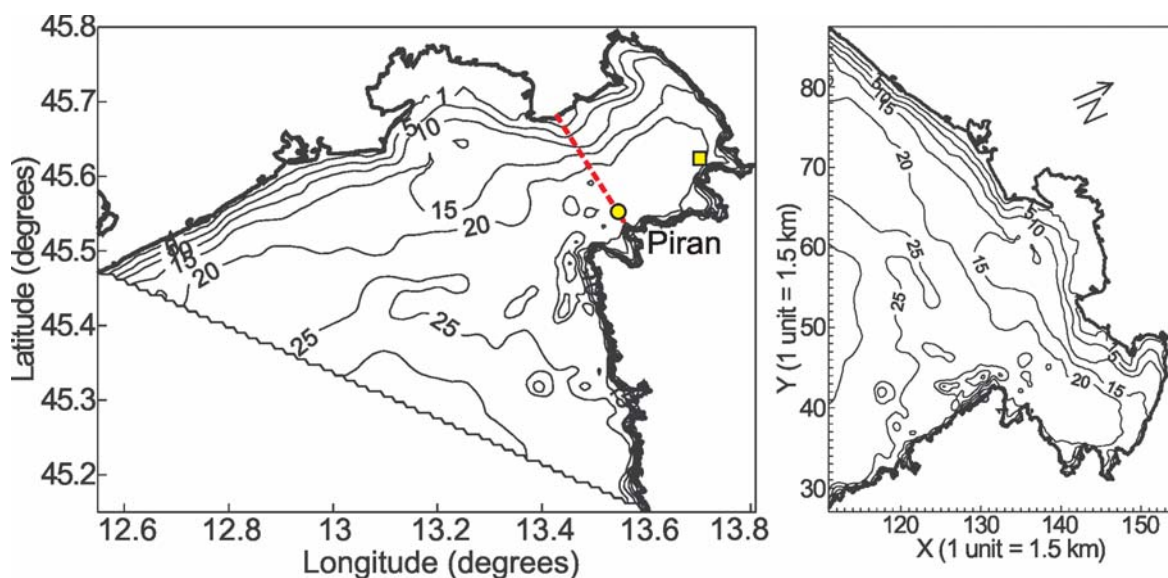


Fig. 1. Model domain of the ACOAST-1.2 model over the northern Adriatic Sea (left). The jagged line is the model open boundary line (OBL), which is placed along the grid line  $x = 111$  of the ASHELF-1 model in which the ACOAST-1.2 model is nested. The model domain is in model coordinates (right); the OBL is at the left-hand side of the model. The depths of the isobaths are in metres. The circle marks the position of the Coastal Oceanographic Station Piran (COSP) and the rectangle station "A" of MOSETTI & MOSETTI (1990)

herein. The model abbreviation means that this is a coastal model of the Adriatic Sea into which another model, the ACOAST-1.1, is to be nested which covers only the interior part of the Gulf of Trieste with a resolution of 0.250 km, run by Istituto Nazionale di Oceanografia e di Geofisica Sperimentale (OGS). The open-boundary line (OBL) coincides with the grid line  $x = 111$  of the ASHELF-1 model. The grid of ACOAST-1.2 was generated from the mesh of the ASHELF-1 model by condensing it by a factor of three to a horizontal resolution of 0.5 km x 0.5 km. Then, the depths of the gridded topography of the northern Adriatic model of tides (TRIM 2D model, MALAČIĆ *et al.*, 2000), which has nearly the same resolution (0.2 nm x 0.2 nm) as the ACOAST-1.2 grid, were re-gridded to this nested grid with inverse distance interpolation. The model grid is composed of 133 x 193 cells in the horizontal, while along the vertical it has 11 sigma-layers. The thickness of the surface and the bottom-most layers increases towards the water column interior in a logarithmic sense.

Seasonal fields of temperature (T) and salinity (S) were generated from an objective analysis of observations (ARTEGANI *et al.*, 1997), and had been first applied in a model of the Adriatic Sea by ZAVATARELLI *et al.* (2002) and also in a model of the northern Adriatic by ZAVATARELLI & PINARDI (2003) in a perpetual year-mode. These fields were interpolated on a three times finer grid than that of the ACOAST-1.2 model. Along the open boundary (OB) line we applied fluxes of momentum, heat and salinity as well as the sea-surface elevation, again obtained from the ASHELF-1 model along its grid line  $x = 111$ . The OB condition of momentum flux was corrected when applied to the three times finer grid (topography) in order to maintain the total prescribed flux (ZAVATARELLI & PINARDI, 2003). A similar procedure was applied to the ECMWF climatology data that force the model at the sea-surface. These data represent wind stress, solar irradiation minus the upward heat flux and evaporation minus precipitation. The surface inputs vary quite smoothly over the model domain (Fig. 2), because the original horizontal resolution of the ECMWF solar heat

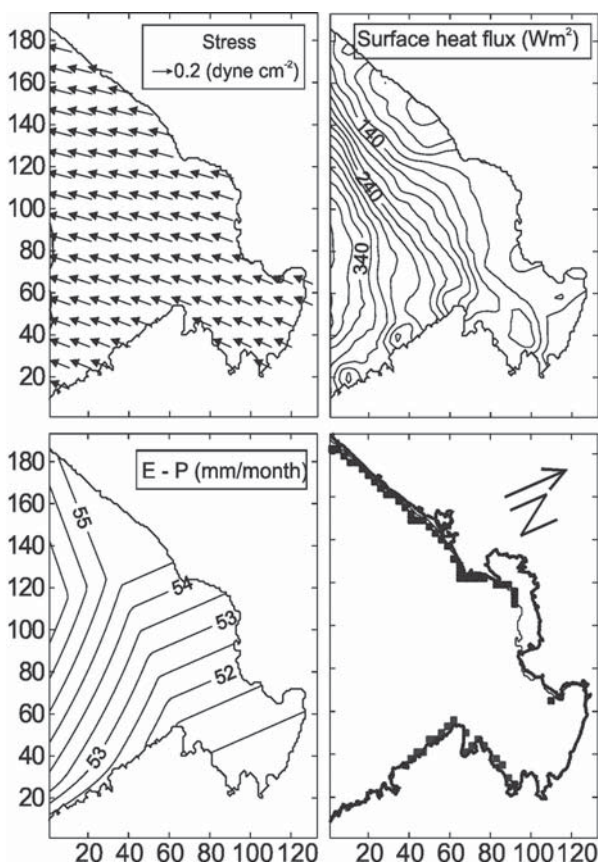


Fig. 2. Wind stress (top left) and the surface heat flux (solar minus upward heat flux, top right), evaporation (E) minus precipitation (P) (bottom left) and locations of freshwater (river) inputs (bottom right) on 10 January of the perpetual year. The monthly data of the wind stress, solar heat flux, and of E-P was obtained from the ECMWF re-analysis, regridded by INGV from Bologna for the ASHELF-1 model (see text), by which the upward heat flux at the surface was calculated. All quantities were interpolated to the ACOAST-1.2 model and linearly interpolated in time between monthly values. The freshwater sources along the coastline are marked with black rectangles. The thin line in the bottom right plot represents the coastline applied in the model, while the thicker line is the coastline GSHHS (Global Self-consistent Hierarchical High-resolution Shorelines), that also marks the Grado lagoon that was not modeled. Numbers along the axes are the values of x and y coordinates in model units (1 model unit equals 0.5 km)

flux and wind stress data was 1.125°, while the upward heat flux was first calculated with the AREG (POM) model of the whole Adriatic Sea (resolution 5 km) and then re-calculated by the ASHELF-1 model (1.5 km resolution). River

inputs are indicated by the reduced salinity around the river outlets (Fig. 2, bottom right).

The reduction of salinity in cells in the upper layer around the outlets depends only on the monthly mean value of the outflow of rivers that fall in the domain of the ACOAST-1.2 model. Since the details of the freshwater fluxes along some parts of the coastline, mostly around lagoons, are unknown, the river fluxes were distributed more evenly over many coastal points (RAICICH, 1996), where the trial and error method was applied in the ASHELF-1 model in order to avoid negative values of salinity.

An analysis of the barotropic transport of the water mass through the vertical plane along the model OB line showed that over the entire perpetual year the barotropic flux is negative with a mean value of  $-5155.2 \text{ m}^3\text{s}^{-1}$  and a standard deviation (SD) that is half of the absolute value of the mean value. In order to maintain the volume of the water mass inside the model domain, the 3D velocities across the vertical plane along the OB line were first corrected so that the total flux through the plane is updated to zero at each time step. First, the 3D velocities across the open boundary plane of a nested model with a finer grid were adapted in order to maintain the total flux given by the nesting model (ZAVATARELLI & PINARDI, 2003). Then, the 3D velocities on the ACOAST-1.2 model grid were adapted for a second time to a constant value so that the total flux throughout the open boundary plane is equal to zero (MARCHESIELLO *et al.*, 2001). Finally, the outward radiation condition was applied for the depth-averaged velocity. Simulations have shown that this second modification of the 3D velocities at the OB plane did not affect the circulation qualitatively, and that velocities changed by up to  $2 \cdot 10^{-3} \text{ ms}^{-1}$ . The river inputs were represented by the lower salinity values in the model domain, and were re-gridded to the nested model from the nesting one. They are without mass and momentum added, and the sea-surface elevation was not adapted for the addition of rivers.

Simulations were completed for a typical winter situation, when the stratification is weak and the climatology shows that the bora wind

field is dominant. The numerical model run in 3D mode showed a stable response for runs with the 'external' time step of 10 s, which covers the response of depth integrated motion, and the 'internal' time step of 150 s.

The model simulations were performed for three different cases of initial and surface boundary conditions. In the first case, the T and S fields were held constant and homogenous and their values were equal to the average value of the ASHELF-1 model over the ACOAST-1.2 model domain, that is T (= 7.19 °C) and S (= 36.62 psu). Only wind stress (ECMWF), which originates from the bora wind, was applied at the sea-surface. In the second case, again, only the (bora) wind stress was applied at the sea-surface. However, the re-gridded T and S fields obtained from the ASHELF-1 model were now applied as the initial T and S fields for the 1st model day (zero time) of a perpetual year (360 days). The T and S were passed across the vertical open-boundary plane according to the upstream advection scheme. In the third case, all possible forcing mechanisms were applied at the surface in addition to the wind stress, i.e. the fluxes of heat (latent and sensible heat flux with long wave radiation at the surface, and penetrative solar radiation at depth), and the salinity flux at the surface (evaporation minus precipitation, with the river flux distributed over the coastal grid points at the sea-surface around the river inlets for the nested model grid). Both were corrected so that sea surface salinities are consistent with the seasonal climatology (observations) and excessive freshening of the basin is avoided (ZAVATARELLI & PINARDI, 2003). The initial fields of T and S were the same as those for the second case. In all three cases the OB condition for velocity was the same (described previously).

## MODEL RESULTS

Distribution of the sea-surface elevation (SSE) during the winter period of the perpetual year (Fig. 3) shows that in all three cases the SSE is piled up towards the model OB line, along the axis of the Gulf of Trieste, and



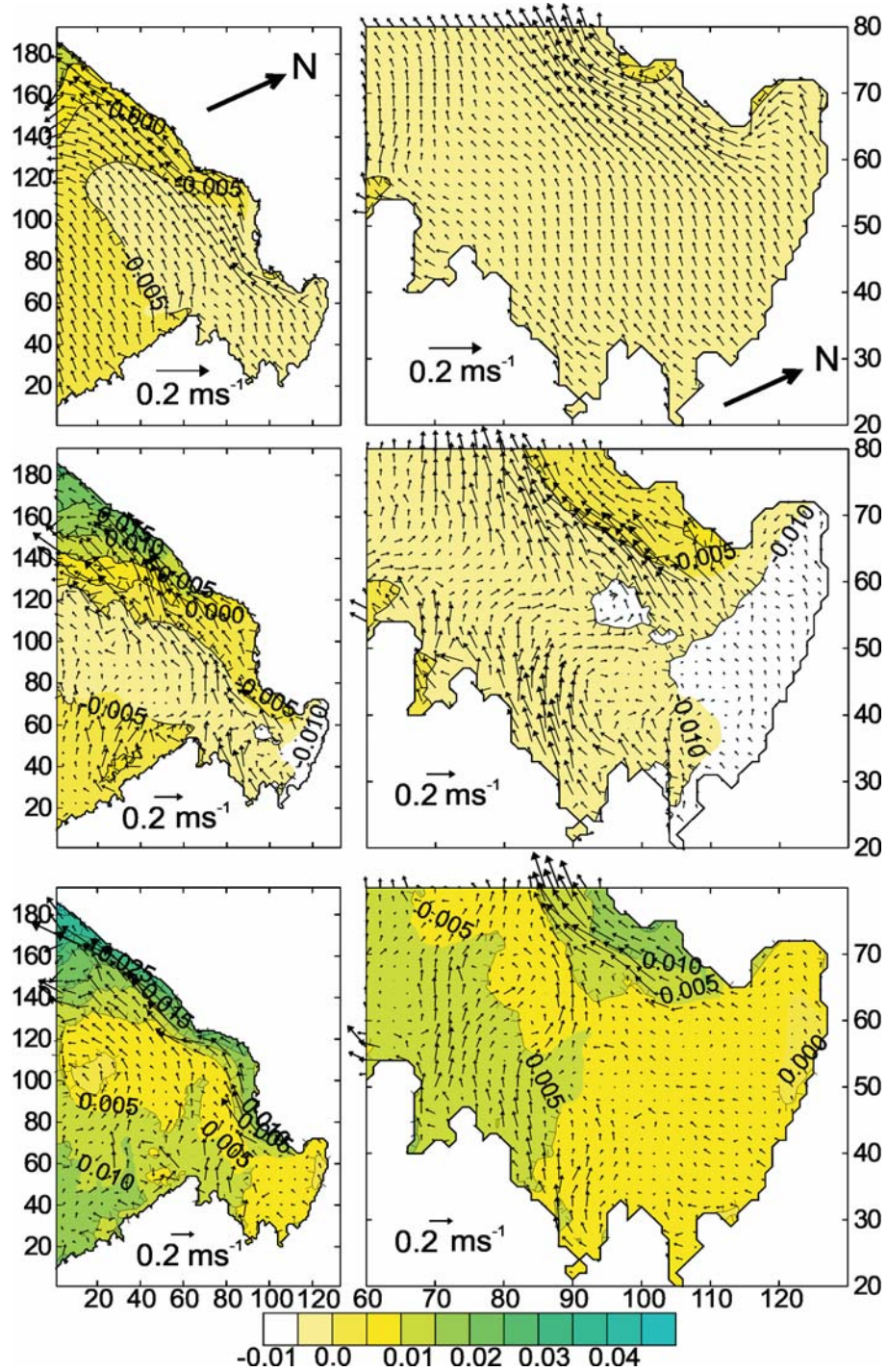


Fig. 3. Sea-surface elevation (colour scale at the bottom of the figure is in meters) and currents at 1 m depth on day 10 of the simulation over the whole model domain (left) and inside the zoomed area of the Gulf of Trieste (right). The top-most plots represent case 1 of the bora wind-driven simulation with homogeneous and constant  $T$  ( $= 7.19^{\circ}\text{C}$ ) and  $S$  ( $= 36.62$  psu). Case 2 (middle) has the same bora wind forcing without any other fluxes at the surface, but with varying  $T$  and  $S$  that were initialised with the re-gridded values of the ASHELF-1 model at time zero. The freshwater sources are invoked through the cells of lower salinity along the coastline (see Fig. 2, bottom right). OB conditions for  $T$  and  $S$  also vary. Case 3 (bottom) is similar to case 2, except for the addition of the fluxes of heat and salt at the surface (ZAVATARELLI & PINARDI, 2003). The same OB condition for velocity was applied in all three cases (see text). Only every sixth vector of velocity is presented for clarity on the left plots, and every second vector (resolution of 1 km) on the right plots

increases especially towards the northwestern corner between the OB line and the Italian coastline. This pattern is mostly governed by the OB conditions and is also seen when only bora wind forcing is present (Fig. 3, top line). It agrees with the idea that bora wind forcing piles up the SSE from the Gulf's interior towards the Venice lagoon, which is outside the model domain (westward of the OB line). Currents at 1 m depth generally follow the wind stress, being enhanced in a shallow strip along the Italian coastline. The variability of the T and S fields (Fig. 3, second row) increases the gradient of SSE across the Gulf's axis, deepening the 'trough' of the SSE that extends out from the Gulf. The core of maximum surface outflow no longer extends towards the Italian coastline near the OB line, but has moved towards the Gulf's center, several miles offshore inside the Gulf (right plot), and up to ten miles offshore outside the Gulf. The inclusion of heat and salinity fluxes and river runoffs (through lower salinity), however, adds small-scale variabilities which manifest on SSE (Fig. 3, bottom plots) and on currents, which follow this redistribution of SSE, and is therefore more complicated: in front of, and inside, the Gulf there is a flow from the southern (Slovenian) boundary towards the northern (Italian) one, across the Gulf's axis, almost as if there is a closed model boundary set up, and the surface flow is released out from the model domain only along the northern coastline. Close to the eastern boundary, inside the Gulf near the Port of Trieste, there is a relatively large area of weak currents at the surface, which contradicts observations (MALAČIČ *et al.*, 1999).

The pressure gradient caused by the piling up of the water surface from the Gulf of Trieste towards the Venice lagoon is present at depth as well and there it creates the counter-current, which conserves the water mass inside the basin (Fig. 4, right plots).

When T and S are allowed to vary in space and time (case 2), up to three anticyclonic vortices are present inside the Gulf, along the southern half of the Gulf's interior (middle of Fig. 4 and top of Fig. 5), almost down to the bottom. Their diameters vary from 5-10 km.

However, when the fluxes of heat and salinity are considered (case 3, bottom of Figs. 4 and 5), three anticyclonic vortices are replaced by one less distinctive cyclonic vortex at depth in the middle of the southern side of the Gulf. This makes the vortices obtained in case 2 more questionable as a pattern for the circulation during the winter period.

Fig. 6 depicts the distribution of the flow across the line Grado-Piran at the Gulf's entrance. We define the inflow velocity as the velocity component along the axis of the Gulf, which is oriented towards the Gulf's interior.

In case 1 (top) the pattern is clear: strong outflow (negative velocities) in the shallow part near Grado (northern side) and in the thin surface layer over the central and southern part of the profile, where at depth there is a weaker, yet consistent inflow. In case 2 (middle plot) and case 3 (bottom plot) the situation is not so simple and clear. While in case 2 there is still a strong outflow confined to the region near Grado, there is also a weak outflow in the southern part of the Gulf that spreads toward the bottom. In case 3 the situation looks even more complicated since the outflow near the northern side of the transect is no longer confined to the very shallow areas, and the vertical strip of the outflow in the southern part of the transect is narrower than that in case 2 and is bounded by the inflow to its left and right. In both case 2 and case 3 there is an inflow in the central part of the Gulf that extends from the surface towards the bottom.

Finally, a preliminary comparison of model currents with the currents which were observed using the coastal oceanographic buoy at Piran (COSP) is presented in Fig. 7 (see Fig. 4, top left, for the position of the buoy). In the model bora-wind stress  $(\tau_E, \tau_N)/\rho$  ( $\rho$  is the density of the sea-water) was applied at the location of COSP at a standard height of 10 m above the mean sea-level, with a value around  $(-1.22 \cdot 10^{-5}, -9.66 \cdot 10^{-6}) \text{ m}^2\text{s}^{-2}$  that varies by about 6% in magnitude during the run of 10 days.

The observed profile of inflow velocity shows a strong outflow near the surface and an inflow at all depths. Although the values near the surface need to be accepted with care



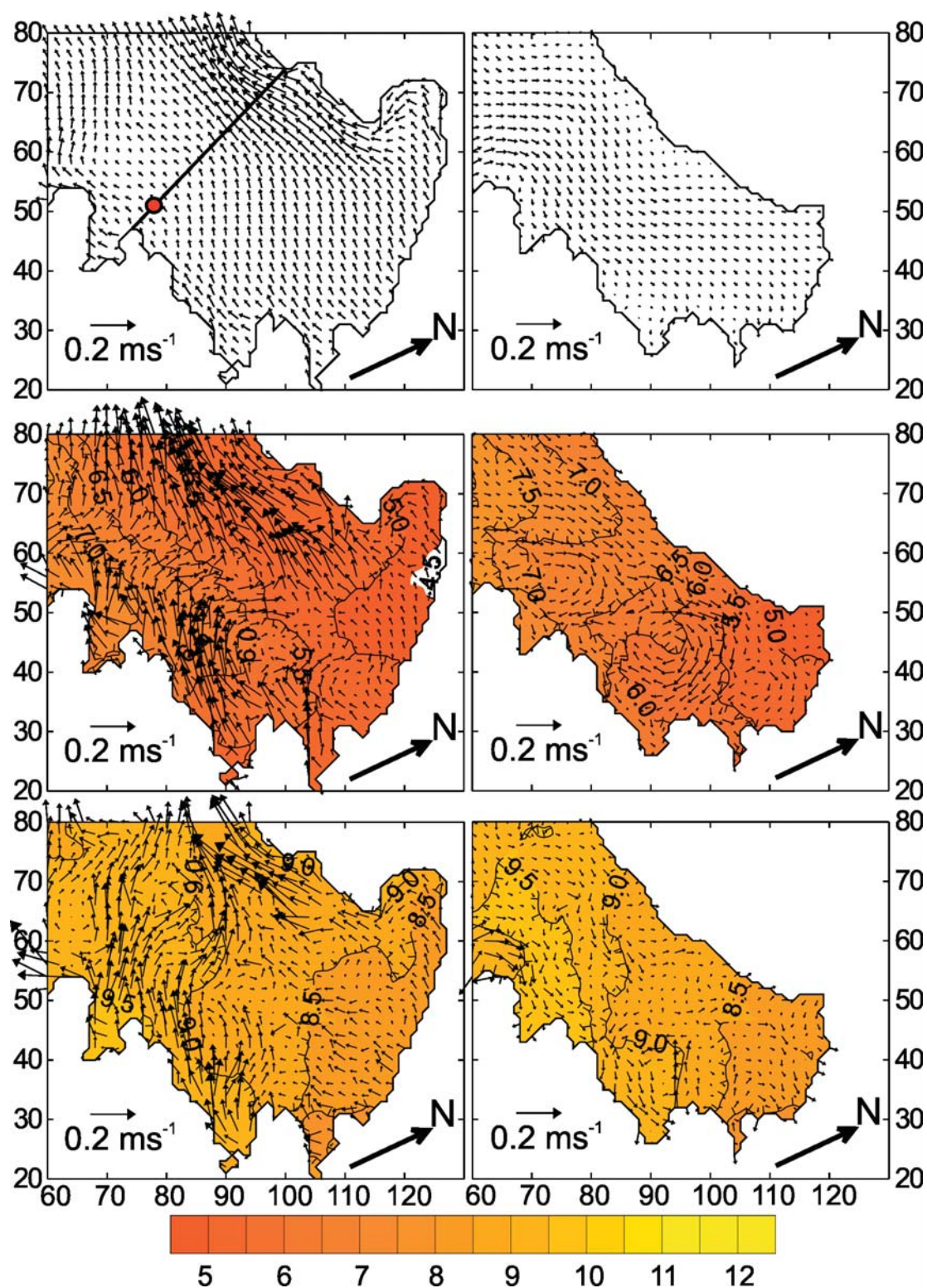


Fig. 4. Currents and temperature inside the Gulf of Trieste at a depth of 1 m (left) and at a depth of 15 m (right) on day 10 of the perpetual year. Cases 1-3 follow from top to bottom, similar to the arrangement in Fig. 3. The line (top left figure) of the profile that closes the Gulf between Grado and Piran is marked together with the position (full circle) of the COSP. The colour scale at the bottom is for the temperature in °C

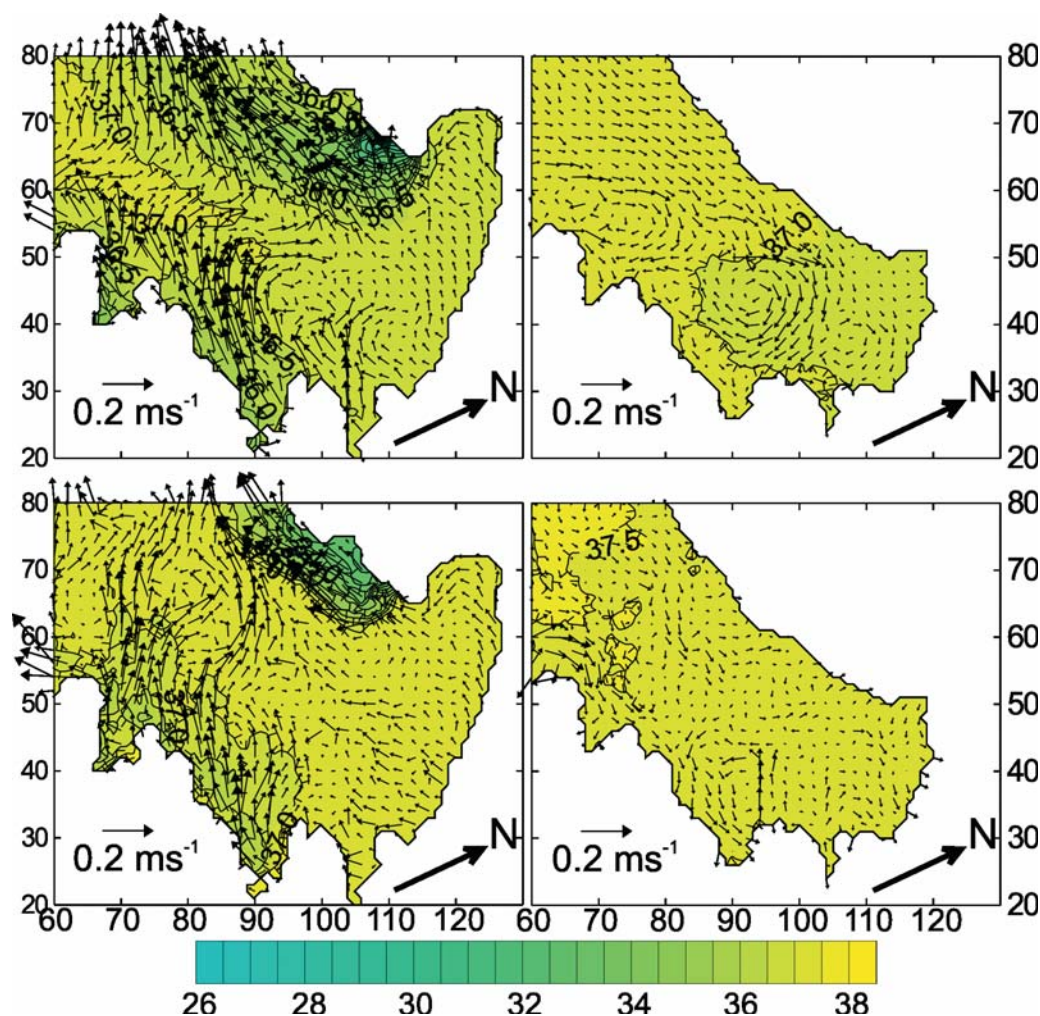


Fig. 5. Similar to Fig. 4, except that case 1 is omitted and the distribution of salinity replaces that of temperature. The model run for case 2 is shown in plots in the top row and for case 3 in the plots of the bottom row. Left plots are for a depth of 1 m, right for a depth of 15 m. The colour scale is in psu

due to the effect of surface waves, this profile makes sense as it is the only measured velocity profile along the southern side of the Gulf thus far. The magnitude of the above-mentioned wind stress (momentum flux)  $\tau/\rho = 1.556 \cdot 10^{-5} \text{ m}^2\text{s}^{-2}$  just below the sea-surface corresponds to a wind speed of around  $3.45 \text{ ms}^{-1}$  (KONDO, 1975) at 10 m height. In case 1 (rectangles), and also in case 3 (diamonds) the model simulations produced a vertical profile of inflow velocity that qualitatively matches the observations, although there is different scaling because of different wind speeds and inclusion of heat fluxes at the sea-surface with the spatiotemporal variability of T and S. During the period of 5-15 January

2003 bora wind at the buoy had a mean speed of  $8.2 \text{ ms}^{-1}$  (most frequent direction of  $63^\circ$ ) and SD of  $5.6 \text{ ms}^{-1}$  at a height of 5 m above the sea-level. This corresponds (KONDO, 1975) to a wind speed of  $8.85 \text{ ms}^{-1}$  at a height of 10 m above the sea level and a momentum flux of  $1.36 \cdot 10^{-4} \text{ m}^2\text{s}^{-2}$ , or about 8.7 times greater than that applied in the model run. Therefore, it is expected that at the position of the coastal buoy the modeled velocities at depths below the surface outflow layer would be smaller than those observed. When the vertical heat and salinity fluxes were ignored (case 2) the vertical profile of modeled inflow (full circles) does not match the observed one.



Fig. 6. Distribution of the normal flow through the transect from Grado ( $x = 0$ ) to Piran ( $x = 21.5$  km), denoting the entrance into the Gulf of Trieste (see Fig. 4, top left plot). Top plot represents the wind-driven flow (case 1), the plot in the middle shows the results of the model run in case 2, and the bottom plot in case 3. The colour scale is in  $\text{ms}^{-1}$

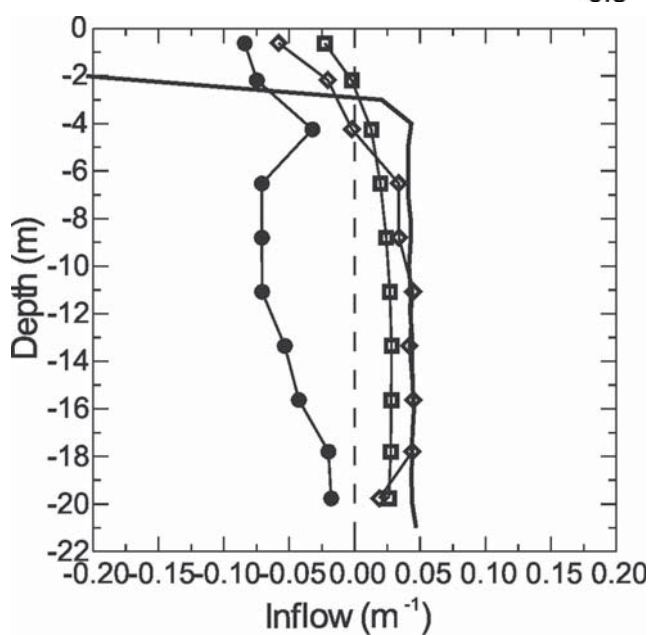
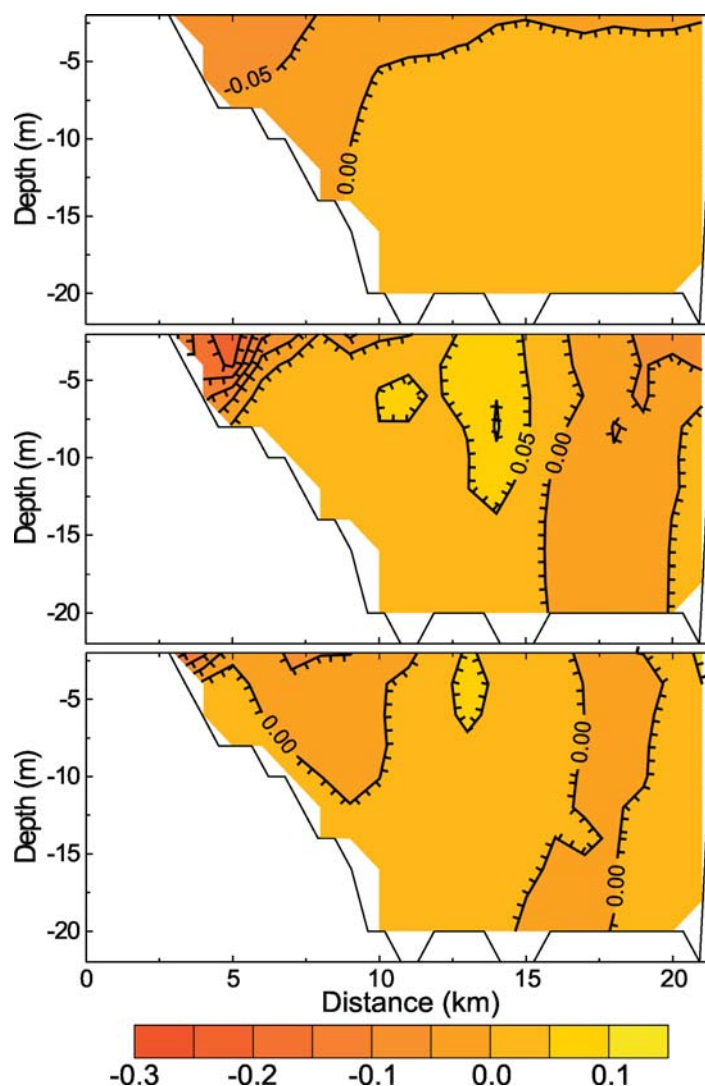


Fig. 7. Vertical profiles of the inflow current (see the definition in the text) at the location of COSP (see Fig. 4, top left, for its position). The full line presents the average inflow current from 5-15 January 2003, measured by the bottom mounted ADCP below the coastal oceanographic buoy during prolonged bora wind. Vertical profiles of inflow model velocities are added for case 1 (rectangles), case 2 (full circles), and for case 3 (diamonds)

## DISCUSSION AND CONCLUSIONS

Three cases of model simulations of winter circulation showed interesting results. The three nearly barotropic anticyclonic vortices in case 2 are dubious: they may indicate that careless use of the T, S and velocity fields, interpolated from the coarser nesting model as the initial fields in the nested model, may have severe consequences if they are not introduced in the model together with the fluxes of heat (and salinity) at the sea surface and at depth (solar radiation). The surface fluxes of heat and salinity, together with penetrative solar radiation, certainly effect weakening in the initial T and S gradients and disrupt the anticyclonic structures. However, many physical mechanisms, related to the variability of all fields and fluxes at the surface, are not yet understood, e.g. the strips of the inflow as well as of the outflow in the southern

part of the Gulf's entrance and the cyclonic structure in the central part at the southern side of the Gulf's interior. They must be explored in the future. However, the model results are plausible and generally acceptable in the case of wind driven circulation (case 1). They show an outflow along the northern (Italian) coastline and in the surface layer all over the Gulf, while there is an inflow at depth in the central and southern sides of the Gulf. This general winter pattern is modified with the variability of T and S caused by their vertical fluxes.

## ACKNOWLEDGEMENTS

This work was supported by the Italian Ministry for the Environment and Territory through the ADRICOSM project, and by the Ministry of Education, Science and Sport of Slovenia (contract no. L1-5289).

## REFERENCES

- ARTEGIANI, A., D. BREGANT, E. PASCHINI, N. PINARDI, F. RAICICH & A. RUSSO. 1997. The Adriatic Sea general circulation. Part II: Baroclinic circulation structure. *J. Phys. Oceanogr.*, 27: 1515-1532.
- KONDO, J. 1975. Air-sea bulk transfer coefficients in diabatic conditions. *Boundary Layer Meteorology*, 9: 91-112.
- MALAČIČ, V. & B. PETELIN. 2001. Regional studies. Gulf of Trieste. In: B. Cushman-Roisin, M. Gačić, P.M. Poulain & A. Artegiani. (Editors). *Physical Oceanography of the Adriatic Sea. Past. Present and Future*. Kluwer Academic Publishers, Dordrecht, pp. 167-181.
- MALAČIČ, V., M. CELIO & J.-J. NAUDIN. 1999. Dynamics of the surface water in the Gulf of Trieste (Northern Adriatic) during drifting experiments. In: T.S. Hopkins, A. Artegiani, G. Cauwet, D. Degobbis & A. Malej (Editors). *Ecosystem Research*, No. 32. The Adriatic Sea (EUR 18834). European Community, pp. 117-125.
- MALAČIČ, V., D. VIEZZOLI & B. CUSHMAN-ROISIN. 2000. Tidal dynamics in the northern Adriatic Sea. *J. Geophys. Res.*, (C), 105: 26,265-26,280.
- MARCHESIELLO, P., J. C. McWILLIAMS & A. SHCHEPETKIN. 2001. Open boundary conditions for long-term integration of regional oceanic models. *Ocean Modeling*, 1-20.
- MOSETTI, F. & N. PURGA. 1983. Free oscillations of the Adriatic Sea. Comparison and discussion of some results by old models and recent experimental investigations. *Boll. Oceanol. Teor. Applic.*, 1: 277-310.
- MOSETTI, F. & P. MOSETTI. 1990. Measurements on wind driven circulation in the North Adriatic Sea. *Boll. Oceanol. Teor. Applic.*, 8: 251-261.
- RAICICH, F. 1996. On the fresh water balance of the Adriatic Sea. *J. Mar. Syst.*, 9: 305-319.
- STRAVISI, F. 1983. The vertical structure annual cycle of the mass field parameters in the

- Gulf of Trieste. *Boll. Oceanol. Teor. Applic.*, 1: 239-250.
- STRAVISI, F., G. PIERI & P. BERGER. 1981. Golfo di Trieste: risultati delle misure correntometriche 1951-1954 (Gulf of Trieste: results of the current measurements 1951-1954). *Boll. Soc. Adriat. Sci.*, 65: 23-35.
- ZAVATARELLI M. & N. PINARDI. 2003. The Adriatic Sea modeling system: a nested approach. *Ann. Geophys.*, 21: 345-364.
- ZAVATARELLI, M., N. PINARDI, V. H. KOURAFALOU & A. MAGGIORE. 2002. Diagnostic and prognostic model studies of the Adriatic Sea circulation. the seasonal variability. *J. Geophys. Res.*, 107, C1, 4/1-4/20.

## Numeričko modeliranje zimske cirkulacije u Tršćanskom zaljevu (sjeverni Jadran)

Vlado MALAČIĆ i Boris PETELIN

*Nacionalni biološki institut, Centar za istraživanje mora Piran, 6330 Piran, Slovenija*

### SAŽETAK

Prikazana je numerička simulacija zimske cirkulacije u Tršćanskom zaljevu i oko njega. ACOAST -1.2 model, baziran na "Princeton Ocean Model" i ugnježđujući se u model šireg područja, daje prihvatljive rezultate za cirkulaciju u zaljevu zimi, kada je bura dominantan vjetar.

Tri numerička eksperimenta s različitim početnim i graničnim uvjetima pokazuju izlaženje vode u cijelom stupcu sjevernog plitkog dijela zaljeva i uz površinu većeg dijela otvorenih granica, te kompenzacijski ulaz u donjem sloju središnjeg i južnog dijela. Promjene u poljima temperature i slanosti povezane s vertikalnim protocima topline i soli definiraju ovu kompleksnu sliku cirkulacije.

**Ključne riječi:** Jadransko more, Tršćanski zaljev, numeričko modeliranje, priobalna hidrodinamika, struje uzrokovane vjetrom